Electronic Supplementary Material (ESI) for Inorganic Chemistry Frontiers.


# Hysteretic Magnetism-Dielectricity Switching in 2D Hofmann Type Spin-Crossover Compounds

Nian-Tao Yao,[a,b] Meng-Jia Shang,[a] Han-Han Lu,[a] Liu Qiang,[a] Wen Wen,[a] Shi-Hui Zhang,[a] Liang Zhao,[a] Oshio Hiroki [a],Yin-Shan Meng*[a] and Tao Liu*[a]

[a] *State Key Laboratory of Fine Chemicals, Frontier Science Center for Smart Materials, School of Chemical Engineering, Dalian University of Technology, 2 Linggong Road, Dalian 116024, China*

[b] *School of Chemistry and Chemical Engineering, Liaocheng University, Liao Cheng, 252059, China*

*Corresponding authors. Email: mengys@dlut.edu.cn; liutao@dlut.edu.cn

# Contents

**Table S1.** Crystal data and structure refinements for compound **1**

| T/K | 210 K | 130 K |
|---|---|---|
| Formula | $C_{32}H_{20}FePtN_8S_2$ | $C_{32}H_{20}FePtN_8S_2$ |
| CCDC | 2115656 | 2115657 |
| Fw | 831.62 | 831.62 |
| Crystal system | Triclinic | Triclinic |
| Space group | $P\bar{1}$ | $P\bar{1}$ |
| *a* (Å) | 9.9135(18) | 9.5956(5) |
| *b* (Å) | 10.0537(19) | 9.8221(6) |
| *c* (Å) | 10.0697(18) | 9.9198(6) |
| *α* (°) | 62.077(5) | 70.656(2) |
| *β* (°) | 66.508(5) | 62.833(2) |
| *γ* (°) | 83.810(5) | 86.684(2) |
| *V* (Å$^3$) | 809.4(3) | 779.96(8) |
| *Z* | 1 | 1 |
| $\rho_{calc}$ (g/cm$^3$) | 1.706 | 1.771 |
| *F* (000) | 404.0 | 404.0 |
| Reflections collected | 14042 | 18160 |
| Unique reflections ($R_{int}$) | 0.0304 | 0.0513 |
| Goodness–of–fit on $F^2$ | 1.097 | 1.064 |
| $R_1$ [$I>2\sigma(I)$][a] | 0.0259 | 0.0226 |
| $wR_2$ [$I>2\sigma(I)$][b] | 0.0633 | 0.0429 |

[a] $R_1 = \Sigma\,(|F_O|-|F_C|) / \Sigma\,|F_O|$; [b] $wR_2 = [\Sigma\, w\,(|F_O|-|F_C|)^2 / \Sigma\, w\, F_O^2]^{1/2}$

**Table. S2** Selected bond distances (Å) and angles (°) for **1** at different states.

| Compound **1**$^{210K}$ | | | |
|---|---|---|---|
| Fe(1)-N(1)$^{2}$ | 2.139(4) | Fe(1)-N(2)$^{4}$ | 2.202(4) |
| Fe(1)-N(1) | 2.139(4) | Fe(1)-N(4)$^{2}$ | 2.207(5) |
| Fe(1)-N(2)$^{3}$ | 2.202(4) | Fe(1)-N(4) | 2.207(5) |
| Fe-N(Av) | 2.183(1) | | |
| N(4)$^{2}$-Fe(1)-N(4) | 180.0 | N(1)-Fe(1)-N(2)$^{4}$ | 90.91(14) |
| N(1)$^{2}$-Fe(1)-N(4) | 91.6(2) | N(1)$^{2}$-Fe(1)-N(2)$^{4}$ | 89.09(14) |
| N(1)-Fe(1)-N(4)$^{2}$ | 91.6(2) | N(2)$^{4}$-Fe(1)-N(4) | 89.09(15) |
| N(1)$^{2}$-Fe(1)-N(4)$^{2}$ | 88.4(2) | N(2)$^{4}$-Fe(1)-N(4)$^{2}$ | 90.91(15) |
| N(1)-Fe(1)-N(4) | 88.4(2) | N(2)$^{3}$-Fe(1)-N(4)$^{2}$ | 89.09(15) |
| N(1)-Fe(1)-N(1)$^{2}$ | 180.0 | N(2)$^{3}$-Fe(1)-N(4) | 90.91(15) |
| N(1)$^{2}$-Fe(1)-N(2)$^{3}$ | 90.91(14) | N(2)$^{3}$-Fe(1)-N(2)$^{4}$ | 180.0 |
| N(1)-Fe(1)-N(2)$^{3}$ | 89.09(14) | | |

$^{1}$2-X, 2-Y, -1-Z; $^{2}$2-X, 2-Y, -Z; $^{3}$1-X, 2-Y, -Z; $^{4}$1+X, +Y, +Z; $^{5}$-1+X, +Y, +Z

| Compound **1**$^{130K}$ | | | |
|---|---|---|---|
| Fe(1)-N(1)$^{2}$ | 1.932(2) | Fe(1)-N(2)$^{4}$ | 2.013(2) |
| Fe(1)-N(1) | 1.932(2) | Fe(1)-N(4)$^{2}$ | 2.011(3) |
| Fe(1)-N(2)$^{3}$ | 2.013(2) | Fe(1)-N(4) | 2.011(3) |
| Fe-N(Av) | 1.985(6) | | |
| N(1)-Fe(1)-N(1)$^{2}$ | 180.0 | N(1)-Fe(1)-N(4) | 91.46(10) |
| N(1)-Fe(1)-N(2)$^{3}$ | 91.93(9) | N(1)-Fe(1)-N(4)$^{2}$ | 88.54(10) |
| N(1)-Fe(1)-N(2)$^{4}$ | 88.07(9) | N(4)$^{2}$-Fe(1)-N(2)$^{3}$ | 89.30(10) |
| N(1)$^{2}$-Fe(1)-N(2)$^{4}$ | 91.93(9) | N(4)$^{2}$-Fe(1)-N(2)$^{3}$ | 90.70(10) |
| N(1)$^{2}$-Fe(1)-N(2)$^{3}$ | 88.07(9) | N(4)-Fe(1)-N(2)$^{4}$ | 89.30(10) |
| N(1)$^{2}$-Fe(1)-N(4) | 88.54(10) | N(4)$^{2}$-Fe(1)-N(2)$^{4}$ | 90.70(10) |
| N(1)$^{2}$-Fe(1)-N(4)$^{2}$ | 91.46(10) | N(4)-Fe(1)-N(4)$^{2}$ | 180.0 |
| N(2)$^{3}$-Fe(1)-N(2)$^{4}$ | 180.0 | | |

$^{1}$-X, 2-Y, 2-Z; $^{2}$-X, 2-Y, 1-Z; $^{3}$-X, 1-Y, 1-Z; $^{4}$+X, 1+Y, +Z; $^{5}$+X, -1+Y, +Z

**Table S3.** Crystal data and structure refinements for compound **2** at different states.

| T/K | 220 K | 100 K |
|---|---|---|
| Formula | $C_{32}H_{20}FePdN_8S_2$ | $C_{32}H_{20}FePdN_8S_2$· |
| CCDC | 2115663 | 2115664 |
| Fw | 742.93 | 742.93 |
| Crystal system | Triclinic | Triclinic |
| Space group | $P\bar{1}$ | $P\bar{1}$ |
| *a* (Å) | 9.9035(5) | 9.711(3) |
| *b* (Å) | 10.0576(6) | 9.829(3) |
| *c* (Å) | 10.0629(5) | 10.012(3) |
| *α* (°) | 62.015(2) | 70.051(5) |
| *β* (°) | 66.630(2) | 86.342(5) |
| *γ* (°) | 83.806(2) | 86.482(3) |
| *V* (Å$^3$) | 808.71(8) | 789.9(5) |
| *Z* | 1 | 1 |
| $\rho_{calc}$ (g/cm$^3$) | 1.525 | 1.562 |
| *F* (000) | 372.0 | 372.0 |
| Reflections collected | 20215 | 4926 |
| Unique reflections ($R_{int}$) | 0.0394 | 0.0433 |
| Goodness–of–fit on $F^2$ | 1.109 | 1.079 |
| $R_1$ [$I>2\sigma(I)$][a] | 0.0485 | 0.0687 |
| $wR_2$ [$I>2\sigma(I)$][b] | 0.1179 | 0.1599 |

[a] $R_1 = \Sigma\,(|F_O|-|F_C|) / \Sigma\,|F_O|$; [b] $wR_2 = [\Sigma\, w\,(|F_O|-|F_C|)^2 / \Sigma\, w\, F_O^2]^{1/2}$

**Table. S4** Selected bond distances (Å) and angles (°) for **2** at different states.

| Compound **2**$^{220K}$ | | | |
|---|---|---|---|
| Fe(1)-N(2)$^3$ | 2.200(6) | Fe(1)-N(2)$^4$ | 2.200(6) |
| Fe(1)-N(4) | 2.201(4) | Fe(1)-N(4)$^2$ | 2.201(4) |
| Fe(1)-N(1)$^2$ | 2.135(5) | Fe(1)-N(1) | 2.135(5) |
| Fe-N(Av) | 2.179(1) | | |
| N(2)$^3$-Fe(1)-N(2)$^4$ | 180.0 | N(1)-Fe(1)-N(2)$^4$ | 88.4(2) |
| N(4)$^2$-Fe(1)-N(2)$^3$ | 89.06(17) | N(1)$^2$-Fe(1)-N(4) | 89.40(16) |
| N(4)-Fe(1)-N(2)$^3$ | 90.94(17) | N(1)-Fe(1)-N(4) | 90.60(16) |
| N(4)$^2$-Fe(1)-N(2)$^4$ | 90.94(17) | N(1)$^2$-Fe(1)-N(4)$^2$ | 90.60(16) |
| N(4)-Fe(1)-N(2)$^4$ | 89.06(17) | N(1)-Fe(1)-N(4)$^2$ | 89.40(16) |
| N(1)-Fe(1)-N(2)$^3$ | 91.6(2) | N(1)-Fe(1)-N(1)$^2$ | 180.0 |
| N(1)$^2$-Fe(1)-N(2)$^4$ | 91.6(2) | N(4)-Fe(1)-N(4)$^2$ | 180.0 |
| N(1)$^2$-Fe(1)-N(2)$^3$ | 88.4(2) | | |

$^1$2-X, -Y, 3-Z; $^2$2-X, -Y, 2-Z; $^3$1-X, -Y, 2-Z; $^4$1+X, +Y, +Z; $^5$-1+X, +Y, +Z

| Compound **2**$^{100K}$ | | | |
|---|---|---|---|
| Fe(1)-N(2)$^2$ | 2.044(5) | Fe(1)-N(2)$^3$ | 2.044(5) |
| Fe(1)-N(4) | 2.048(5) | Fe(1)-N(4)$^4$ | 2.048(5) |
| Fe(1)-N(1)$^4$ | 1.968(5) | Fe(1)-N(1) | 1.968(5) |
| Fe-N(Av) | 2.020(5) | | |
| N(2)$^2$-Fe(1)-N(2)$^3$ | 180.0 | N(1)-Fe(1)-N(2)$^3$ | 88.1(2) |
| N(4)$^4$-Fe(1)-N(2)$^2$ | 89.2(2) | N(1)-Fe(1)-N(4)$^4$ | 88.6(2) |
| N(4)$^4$-Fe(1)-N(2)$^3$ | 90.8(2) | N(1)$^4$-Fe(1)-N(4) | 88.6(2) |
| N(4)-Fe(1)-N(2)$^3$ | 89.2(2) | N(1)-Fe(1)-N(4) | 91.4(2) |
| N(4)-Fe(1)-N(2)$^2$ | 90.8(2) | N(1)$^4$-Fe(1)-N(4)$^4$ | 91.4(2) |
| N(1)$^4$-Fe(1)-N(2)$^2$ | 88.1(2) | N(1)-Fe(1)-N(1)$^4$ | 180.0 |
| N(1)$^4$-Fe(1)-N(2)$^3$ | 91.9(2) | N(4)-Fe(1)-N(4)$^4$ | 180.0 |
| N(1)-Fe(1)-N(2)$^2$ | 91.9(2) | | |

$^1$2-X, -Y, -Z; $^2$2-X,1-Y, 1-Z; $^3$+X, -1+Y, +Z; $^4$2-X, -Y, 1-Z; $^5$+X, 1+Y, +Z

**Table. S5** The distances of C-H···N for **1** and **2** at different temperatures.

| Compound **1** | $C_{13}$-$H_{13}$···$N_3$ (Å) | $C_{13}$-$H_{13}$···$N_5$ (Å) |
|---|---|---|
| 210 K | 2.767 | 2.586 |
| 130 K | 2.507 | 2.493 |
| Compound **2** | $C_{13}$-$H_{13}$···$N_5$ | $C_{13}$-$H_{13}$···$N_3$ |
| 220 K | 2.766 | 2.585 |
| 100 K | 2.511 | 2.536 |

**Table. S6** The parameters for **1** at different temperatures.

| *T* (K) | *a*-axis (Å) | *b*-axis (Å) | *c*-axis (Å) | *V* (Å$^3$) |
|---|---|---|---|---|
| 140 | 9.5796(7) | 9.8072(7) | 9.90921(8) | 776.52(10) |
| 150 | 9.5711(7) | 9.7960(8) | 9.8906(8) | 774.11(11) |
| 155 | 9.5811(7) | 9.8061(7) | 9.9016(7) | 776.71(10) |
| 160 | 9.5853(7) | 9.8100(7) | 9.9074(7) | 777.92(10) |
| 165 | 9.5825(7) | 9.8054(7) | 9.9033(7) | 777.14(10) |
| 170 | 9.5833(7) | 9.8048(7) | 9.9024(8) | 777.14(10) |
| 175 | 9.5866(8) | 9.8062(9) | 9.9053(9) | 777.73(12) |
| 180 | 9.9099(8) | 10.0364(8) | 10.0367(8) | 804.72(11) |
| 190 | 9.9048(12) | 10.0356(13) | 10.0393(12) | 804.35(18) |
| 200 | 9.910(2) | 10.039(2) | 10.043(2) | 805.4(3) |
| 210 | 9.9137(15) | 10.0432(16) | 10.0475(15) | 806.7(2) |
| 200 | 9.9040(14) | 10.0335(14) | 10.0405(14) | 804.4(2) |
| 190 | 9.9093(11) | 10.0408(11) | 10.0434(11) | 805.32(16) |
| 180 | 9.9062(9) | 10.0298(9) | 10.0402(8) | 803.66(12) |
| 175 | 9.9059(7) | 10.0295(8) | 10.0395(7) | 803.44(10) |
| 170 | 9.9049(7) | 10.0283(7) | 10.0390(7) | 803.21(10) |
| 165 | 9.9198(8) | 10.0364(8) | 10.0423(8) | 805.47(11) |
| 160 | 9.5976(7) | 9.8069(8) | 9.8982(8) | 776.87(11) |
| 155 | 9.5943(7) | 9.8105(7) | 9.9020(7) | 777.32(10) |
| 150 | 9.5850(7) | 9.8035(7) | 9.8956(7) | 775.56(10) |
| 145 | 9.5909(7) | 9.8112(7) | 9.9040(8) | 777.32(10) |
| 140 | 9.5876(7) | 9.8087(8) | 9.9003(8) | 776.51(11) |
| 130 | 9.5885(7) | 9.8107(7) | 9.9031(7) | 776.81(10) |

**Table. S7** The parameters for **2** at different temperatures.

| *T* (K) | *a*-axis (Å) | *b*-axis (Å) | *c*-axis (Å) | (Å$^3$) |
|---|---|---|---|---|
| 220 | 9.915(1) | 10.0581(11) | 10.061(1) | 808.84(15) |
| 210 | 9.9234(14) | 10.0617(14) | 10.0626(13) | 809.5(2) |
| 200 | 9.9150(6) | 10.0544(6) | 10.0554(6) | 807.52(9) |
| 195 | 9.9227(9) | 10.0639(9) | 10.0657(9) | 809.38(13) |
| 190 | 9.9232(9) | 10.0619(9) | 10.0633(9) | 808.93(13) |
| 185 | 9.9264(9) | 10.0633(8) | 10.0643(8) | 809.23(12) |
| 180 | 9.9228(8) | 10.0603(8) | 10.0604(8) | 808.25(11) |
| 170 | 9.9184(8) | 10.0536(7) | 10.0569(7) | 806.99(10) |
| 160 | 9.9163(7) | 10.0516(7) | 10.0557(7) | 806.34(10) |
| 155 | 9.6057(9) | 9.8316(10) | 9.9319(9) | 782.80(13) |
| 150 | 9.6012(10) | 9.8273(10) | 9.9263(10) | 781.31(14) |
| 140 | 9.6145(8) | 9.8129(8) | 9.9251(8) | 780.13(11) |
| 150 | 9.6099(8) | 9.8075(8) | 9.9209(8) | 779.19(11) |
| 155 | 9.6170(9) | 9.8133(9) | 9.9259(9) | 780.80(13) |
| 160 | 9.6229(9) | 9.8172(9) | 9.9313(9) | 782.18(13) |
| 170 | 9.5881(11) | 9.8097(10) | 9.9130(12) | 778.91(16) |
| 180 | 9.582(2) | 9.801(2) | 9.897(3) | 775.9(3) |
| 185 | 9.9174(12) | 10.0436(14) | 10.0457(13) | 806.35(19) |
| 190 | 9.9217(13) | 10.0496(15) | 10.0514(14) | 807.8(2) |
| 195 | 9.9248(14) | 10.0552(16) | 10.0560(15) | 808.9(2) |
| 200 | 9.9089(6) | 10.0451(6) | 10.0481(6) | 806.26(9) |
| 205 | 9.9269(6) | 10.0626(6) | 10.0690(6) | 811.10(9) |
| 210 | 9.9292(5) | 10.0682(5) | 10.0710(5) | 812.30(7) |

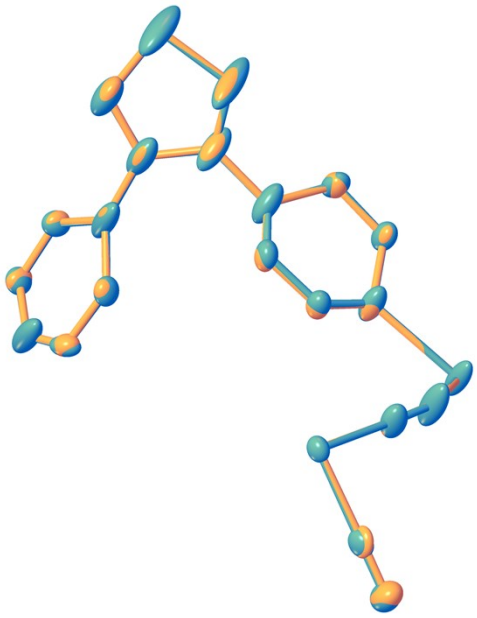

**Fig. S1.** The smallest asymmetric units of compounds **1** (orange) and **2** (grey blue).

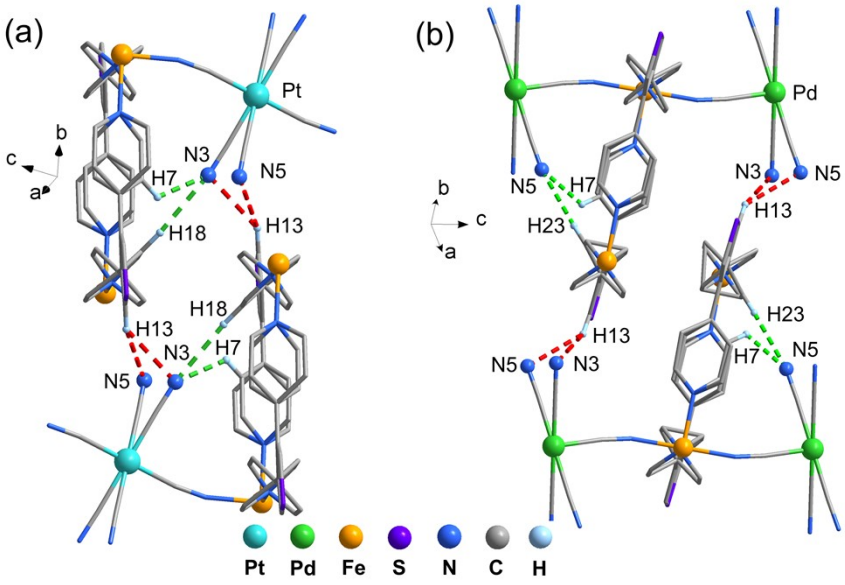


**Fig. S2.** The inter- and intramolecular hydrogen bonds depicted by red and green dash lines for **1** (a) and **2** (b), respectively. Color code: Fe, light orange; Pt, aqua; Pd, green; S, purple; C, grey; N, blue; O, red; H, pale blue.

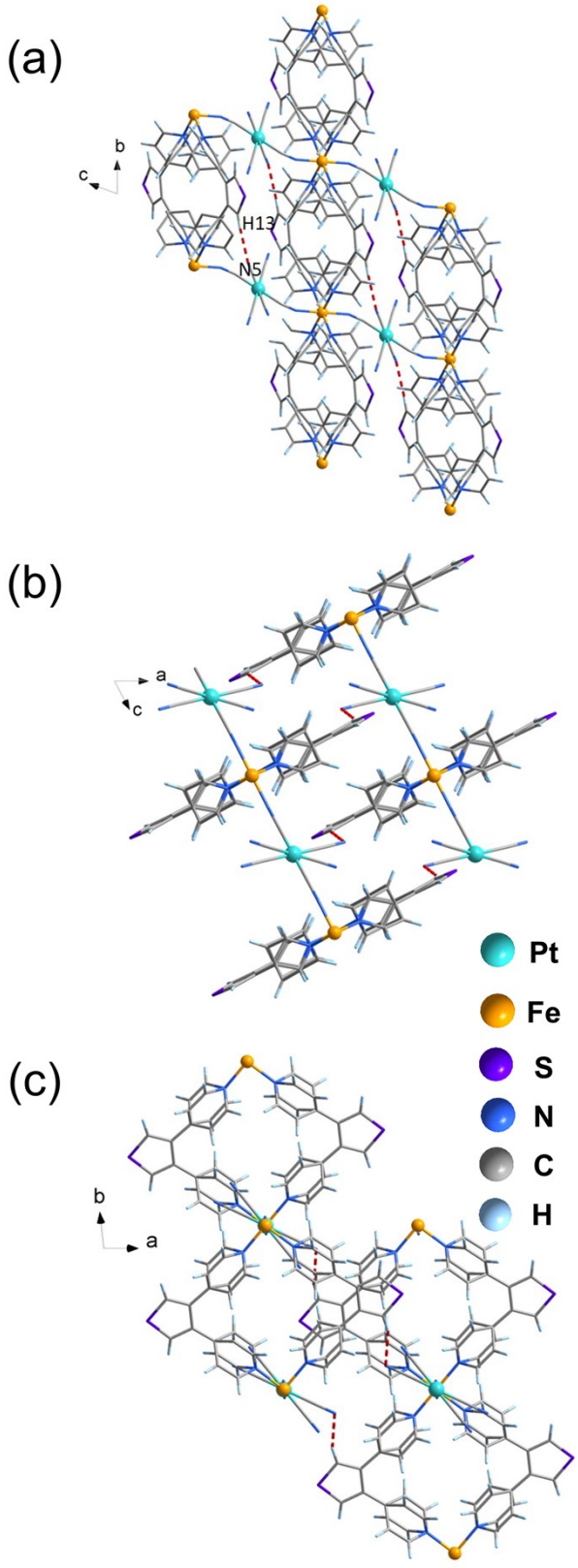


**Fig. S3.** Packing diagrams of compound **1**. Color code: Fe, light orange; Pt, aqua; S, purple; C, grey; N, blue; O, red; H, pale blue. The red dashed lines represent C−H···N hydrogen bonds.

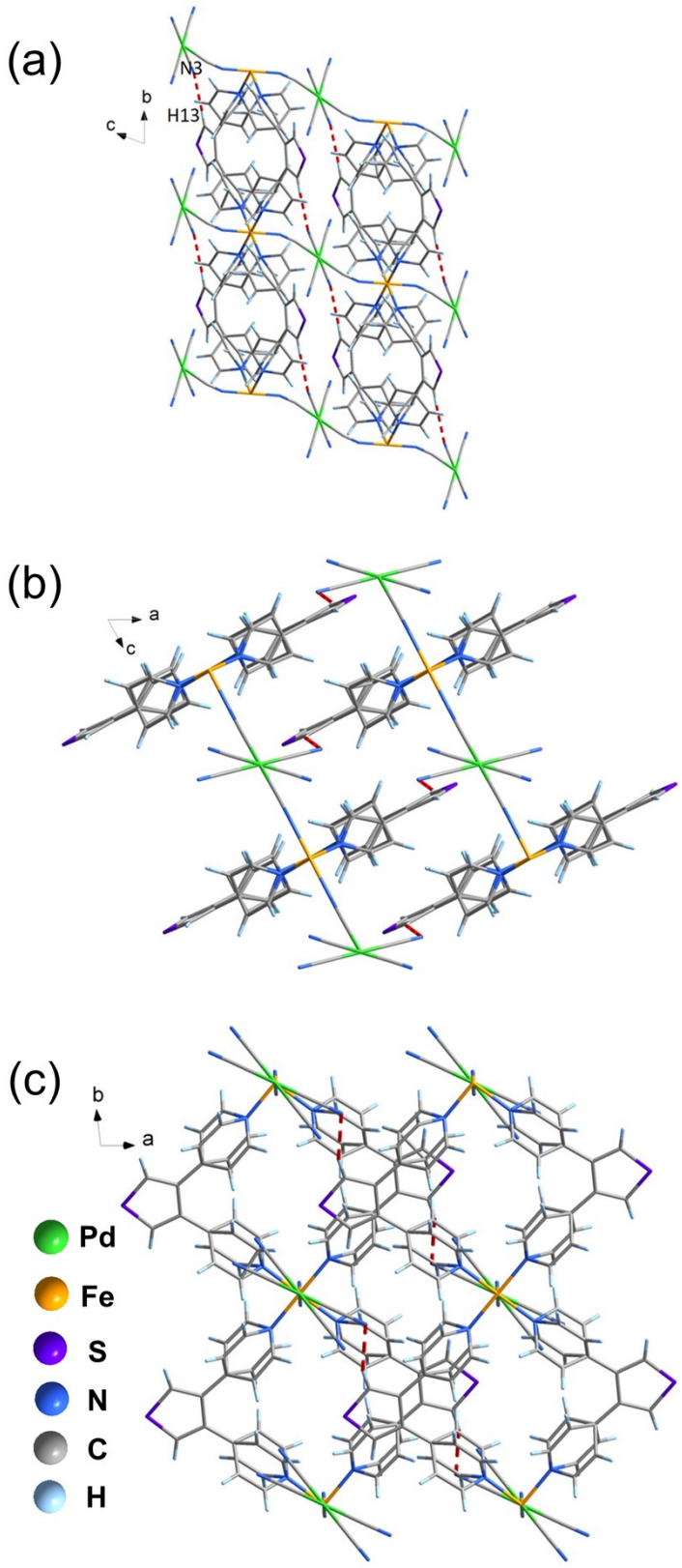


**Fig. S4.** Packing diagrams of compound **2**. Color code: Fe, light orange; Pd, green; S, purple; C, grey; N, blue; O, red; H, pale blue. The red dashed lines represent C−H···N hydrogen bonds.

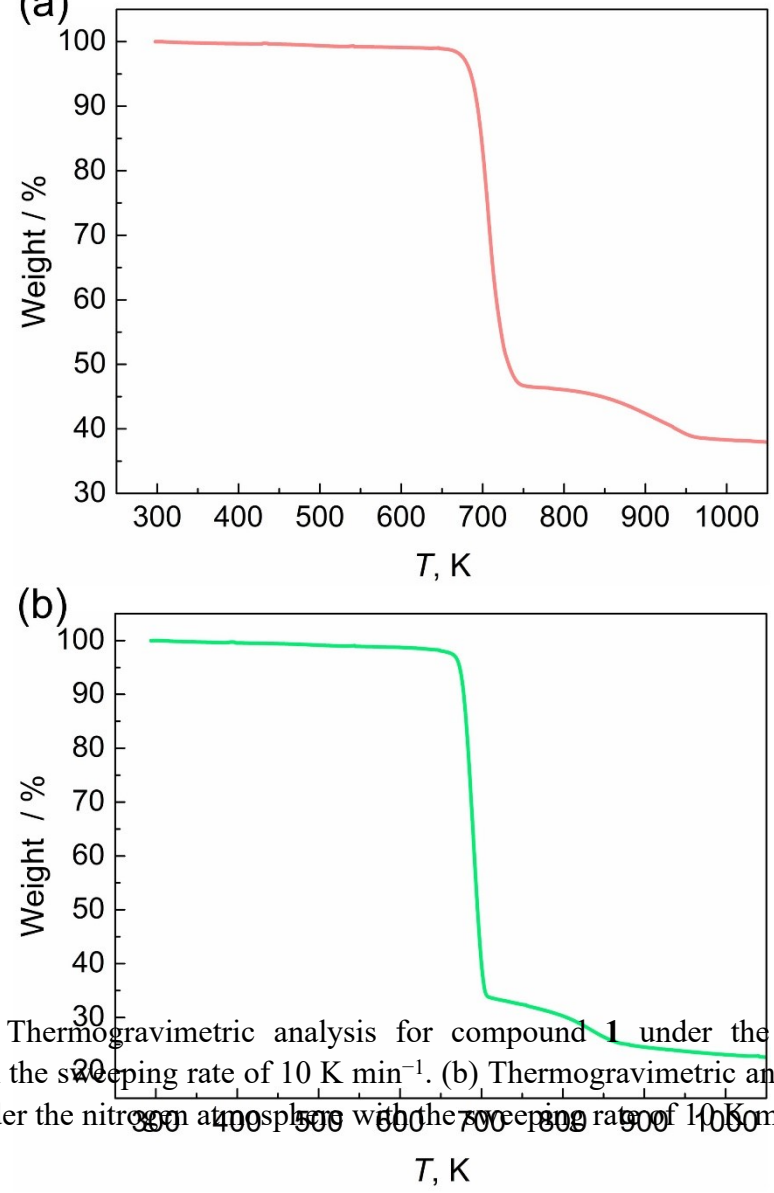


**Fig. S5.** (a) Thermogravimetric analysis for compound **1** under the nitrogen atmosphere with the sweeping rate of 10 K $min^{-1}$. (b) Thermogravimetric analysis for compound **2** under the nitrogen atmosphere with the sweeping rate of 10 K $min^{-1}$.

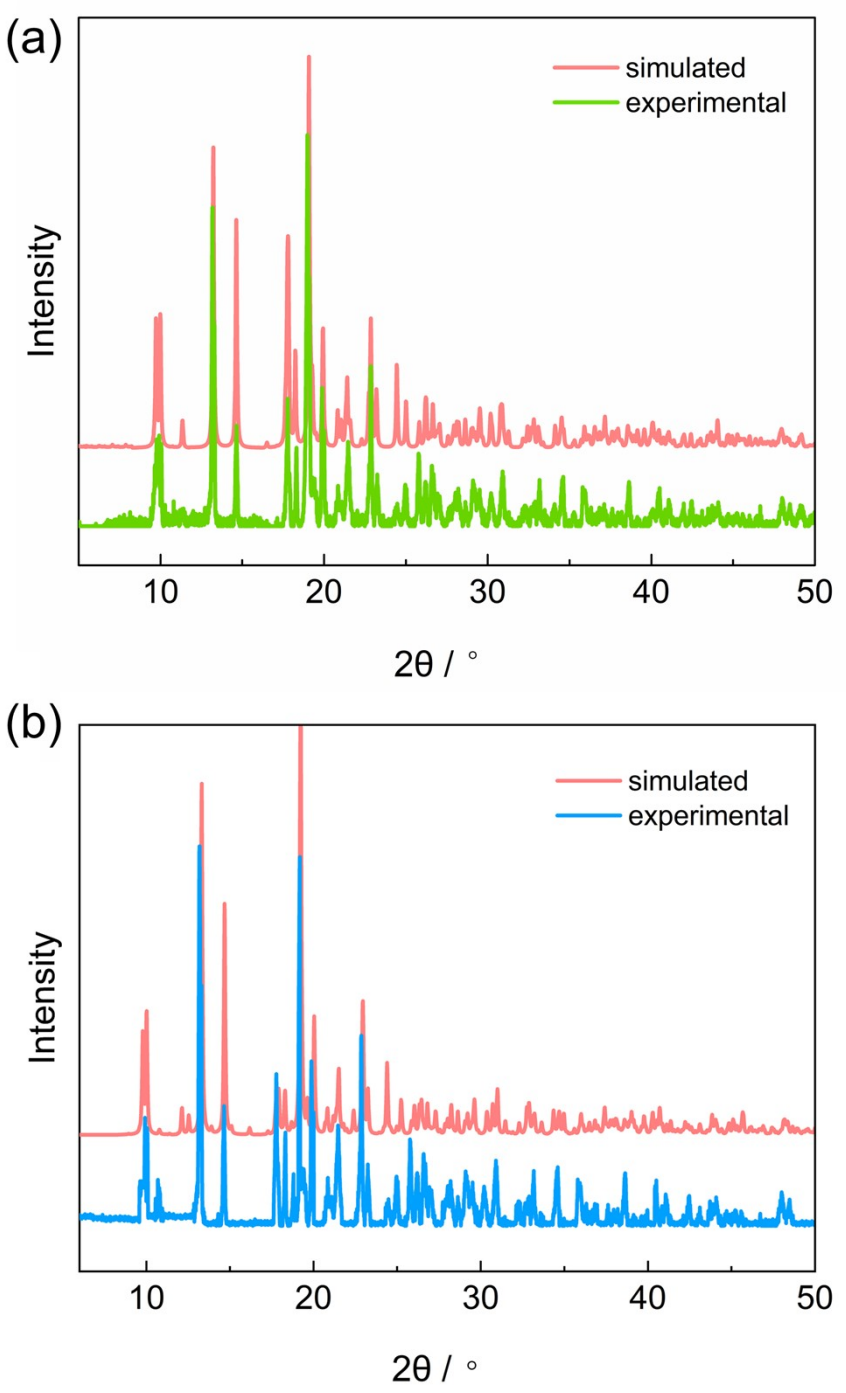


**Fig. S6.** X-ray powder diffraction data for compounds **1 (a)** and **2 (b)** at room temperature. Powder X-ray diffraction (P-XRD) patterns were recorded on a Rigaku Smartlab X-ray Diffractometer utilizing Cu-Kα radiation (λ = 1.54178 Å). The data were represented after the direct background subtraction via MDI Jade6 software.

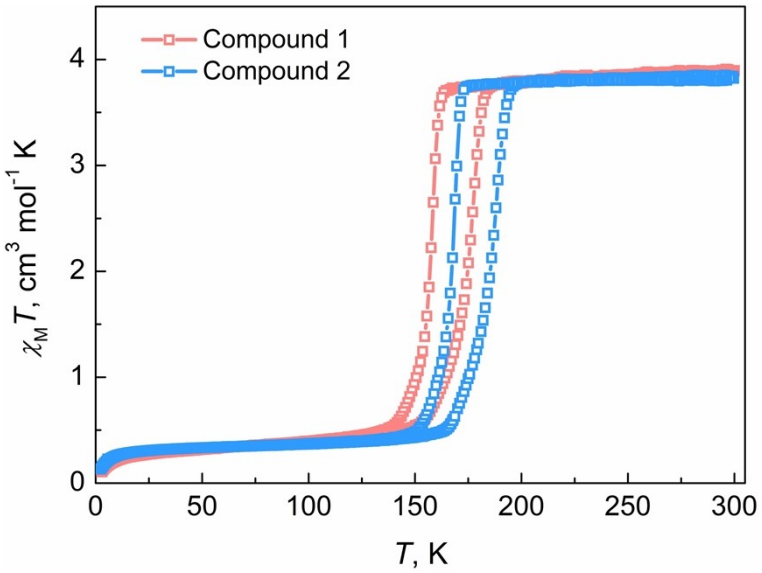


**Fig. S7.** Temperature-dependent susceptibilities of compounds **1** and **2** under applied dc field of 1000 Oe for heating and cooling cycles.

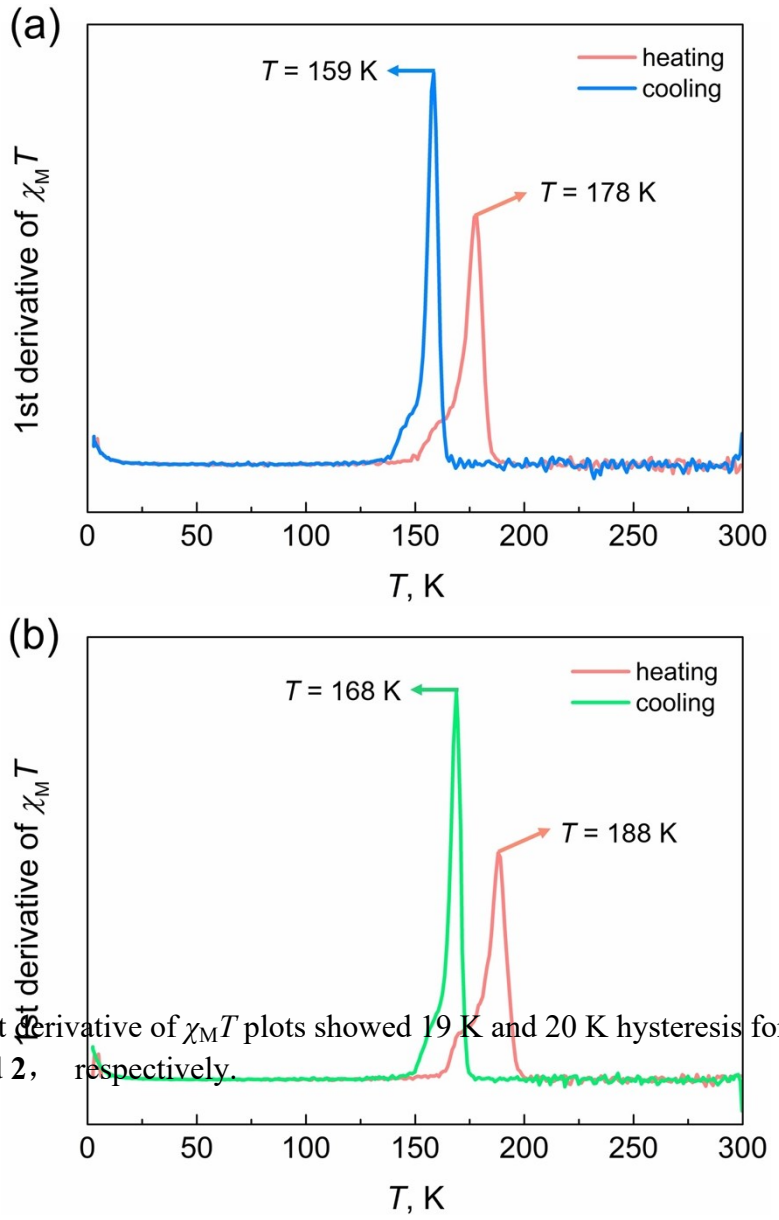


**Fig. S8.** The 1st derivative of $\chi_M T$ plots showed 19 K and 20 K hysteresis for compounds **1** and **2**, respectively.

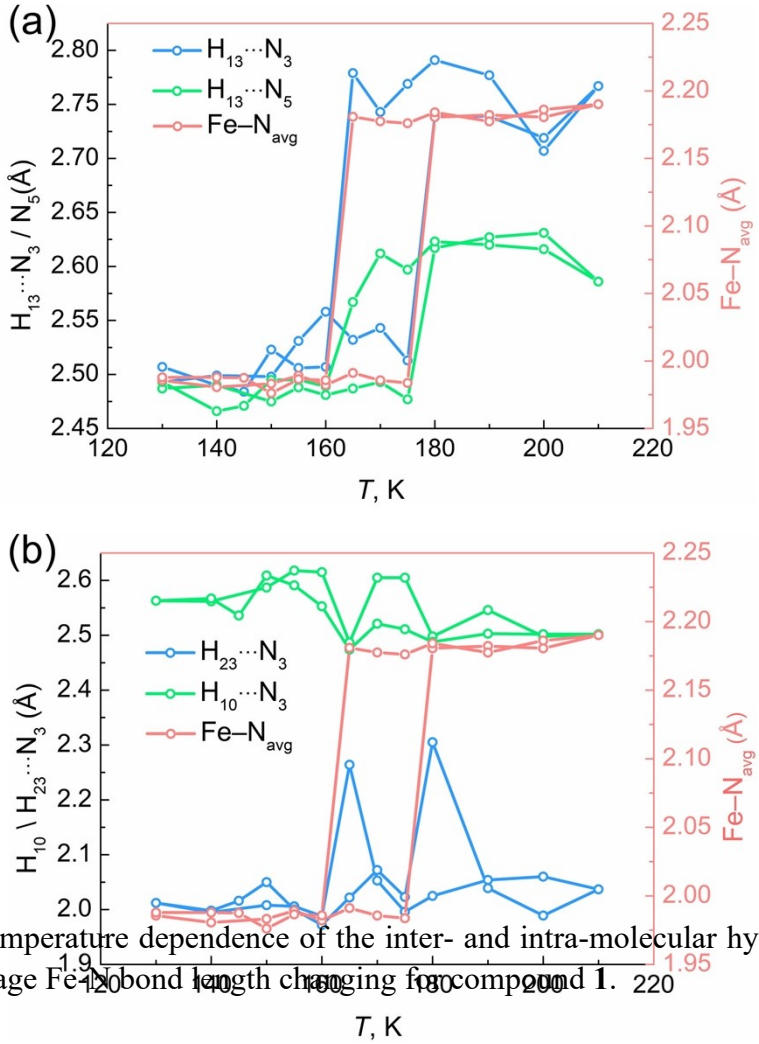


**Fig. S9.** Temperature dependence of the inter- and intra-molecular hydrogen bonds with the average Fe-N bond length changing for compound **1**.

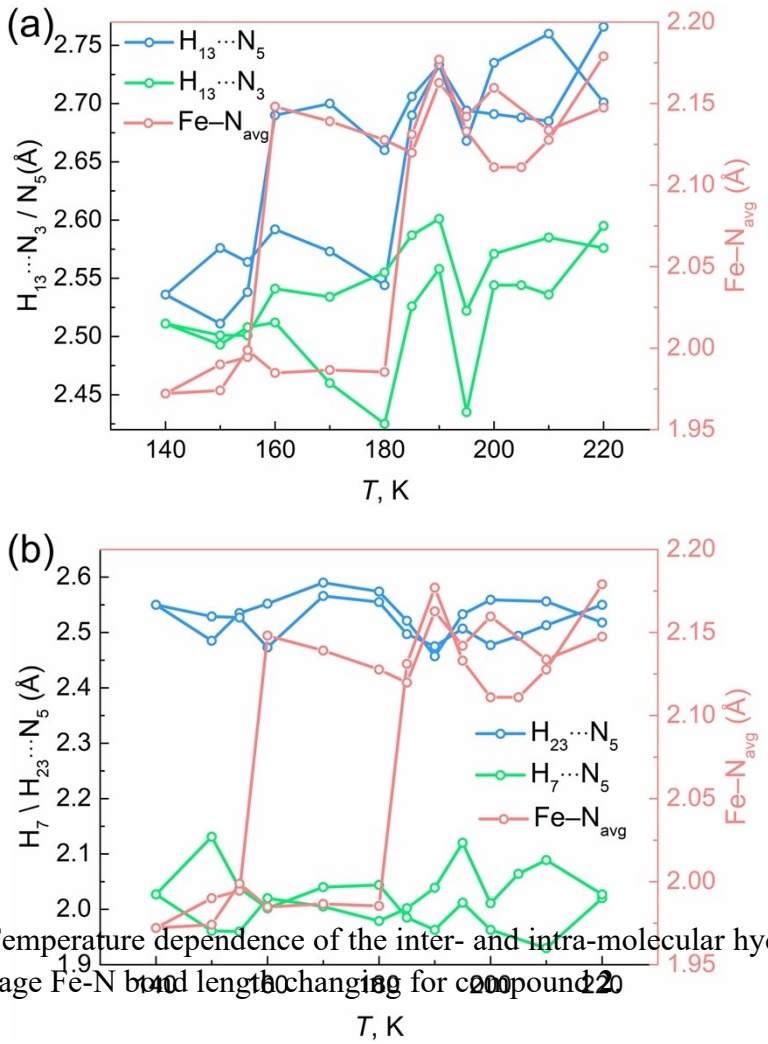


**Fig. S10.** Temperature dependence of the inter- and intra-molecular hydrogen bonds with the average Fe-N bond length changing for compound 2.

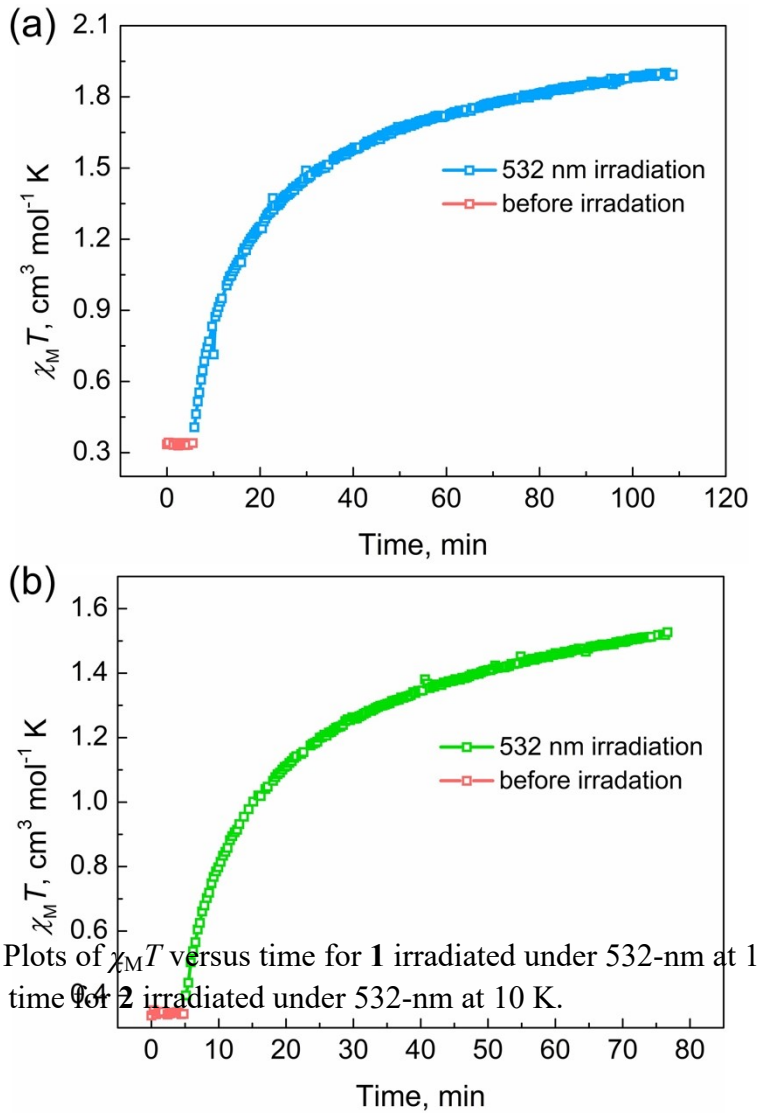


**Fig. S11**. (a) Plots of $\chi_M T$ versus time for **1** irradiated under 532-nm at 10 K. (b) Plots of $\chi_M T$ versus time for **2** irradiated under 532-nm at 10 K.

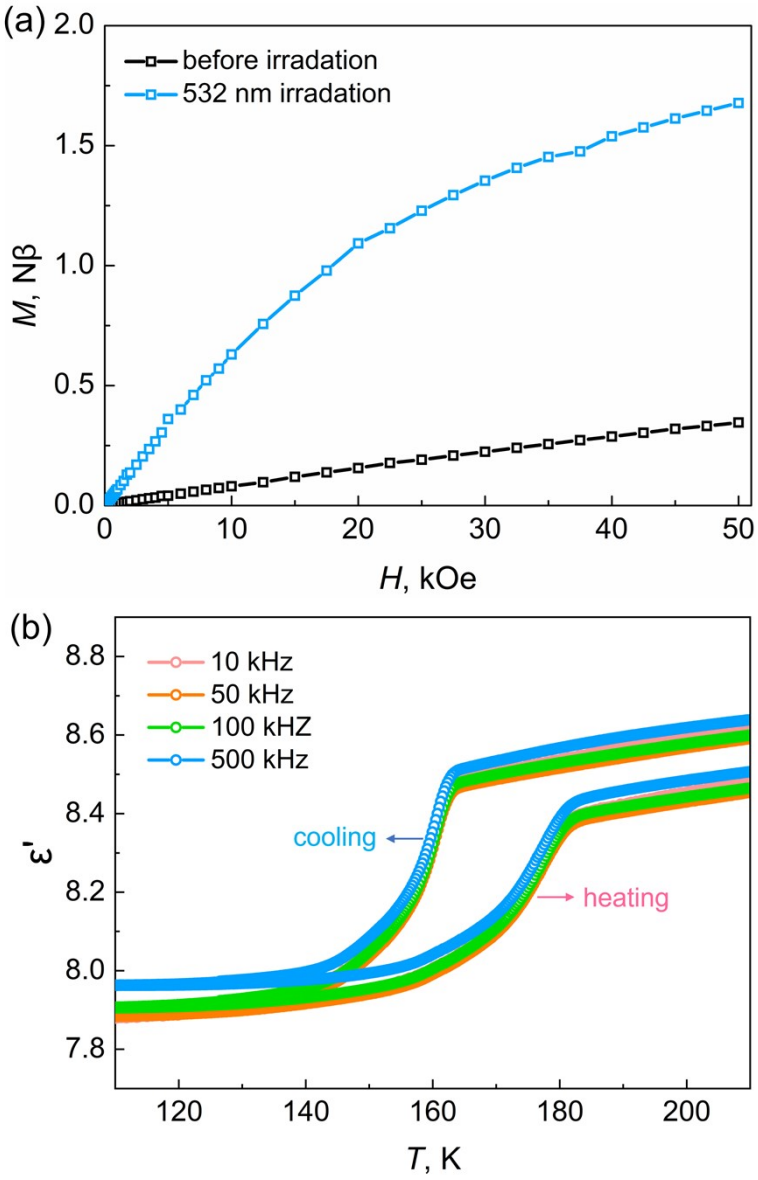


**Fig. S12**. (a) Isothermal magnetization of **1** before and after 532-nm light irradiation. (b) Temperature-dependent ' with different frequencies for the powder-pressed pellet sample of compound **1**.

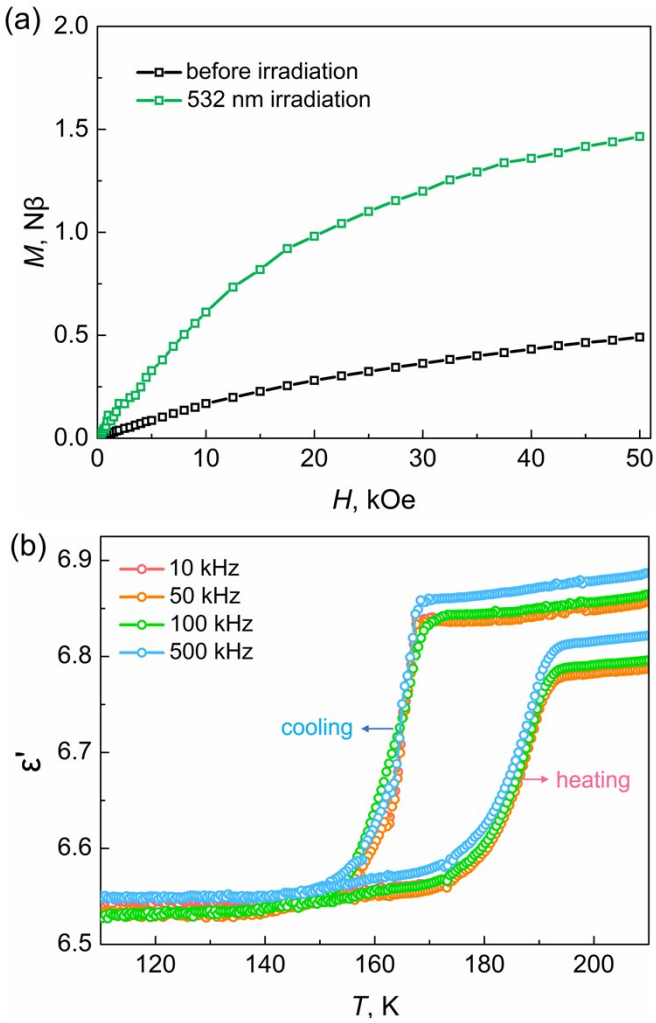


**Fig. S13.** (a) Isothermal magnetization of compound **2** before and after 532 nm light irradiation. (b) Temperature-dependent ' with different frequencies for the powder-pressed pellet sample of compound **2**.

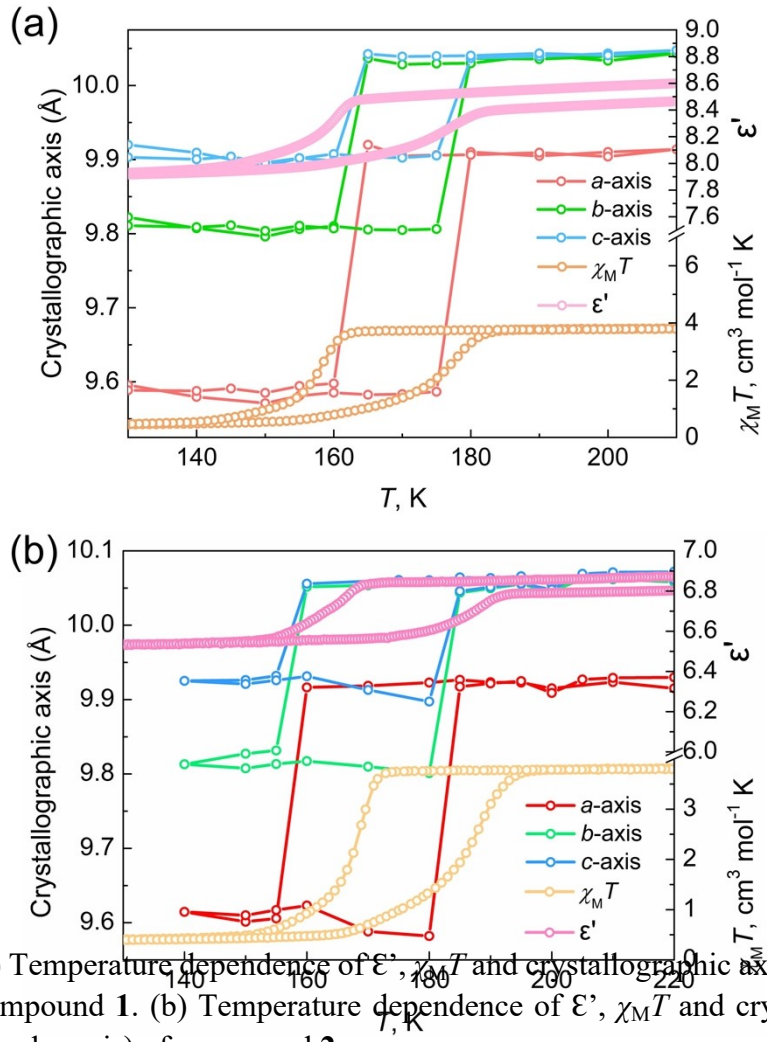


**Fig. S14.** (a) Temperature dependence of Ɛ', $\chi_M T$ and crystallographic axes (a-, b-, and c-axis) of compound **1**. (b) Temperature dependence of Ɛ', $\chi_M T$ and crystallographic axes (a-, b-, and c-axis) of compound **2.**